

ACTIVE CONTROL OF AN INCOMPRESSIBLE AXISYMMETRIC JET USING FLAPSYogesh Singh, David Greenblatt², Christian Navid Nayeri

Christian Oliver Paschereit

christian.nayeri@tu-berlin.deHermann-Föttinger Institute (HFI/ISTA), Technical University Berlin,
Berlin 10623, Germany.²Faculty of Mechanical Engineering, Technion - Israel Institute of Technology,
Technion City - Haifa 3200, Israel.**ABSTRACT**

The near field of an incompressible round jet flow was investigated for generation of streamwise vortices using active flow control. Zero mass-flux perturbations were used to excite the flow. The lip of the jet was equipped with a small flap deflected away from the stream. Effects of changing the flap deflection angle on the flow momentum, streamwise vorticity, circulation and turbulence were studied. The emphasis is being placed on mapping the development of the trailing vortices in order to quantify the mixing achieved.

In the ongoing work, the emphasis is being placed on mapping the development of streamwise vortices generated in order to quantify the mixing achieved. As regards active control, the objective is to investigate experimentally, the concept and principle of mixing between a jet and quiescent fluid using an actively controlled finite-span flap via active flow control. This includes measuring flap loads by means of local surface pressure measurements and measuring the flow field above the flap and in its wake.

INTRODUCTION

The physics of mixing is of great importance in many industrial applications. In engineering flows, the process of mixing governs the amount of energy released in gas turbine combustion chambers, and the level of noise produced by a jet. Most of the mixing requirements are related to the rapidity and spatial uniformity of the mixing process and the cost associated with performing the mixing. The two main and interrelated mechanisms of mixing in turbulent flows are turbulent diffusivity and vorticity. It is widely recognized that a powerful mechanism for enhancing mixing is the generation of strong streamwise vortices. There are a variety of ways in which this idea has been implemented, but the basic concept of utilizing a streamwise vortical structure with its associated cross-stream circulation to augment the rate of mixing is fundamental to all of them.

The manipulation of flowfields by passive devices or the introduction of momentum, or periodic perturbations, is an active area of research. Flow control involves passive or active devices to effect a beneficial change in wall bounded or free-shear flows. Whether the task is to delay/advance transition, to suppress/enhance turbulence or to prevent/provoke separation, useful end results include drag reduction, lift enhancement, mixing augmentation and flow-induced noise suppression.

In the realm of passive devices, vortex generators are often used for separation control [1-3] and also jet noise has been widely controlled by means of chevrons or chevron/tab combinations and non-circular jet geometries [4] in recent years. Much effort has been expended in order to optimize these systems. A negative consequence of successful noise control invariably results in some loss of thrust at cruise conditions. Thus recent work is aimed at applications oriented research using, for example, shape memory alloys to minimize the losses at cruise conditions [5]. Active flow control methods involve introducing perturbations to the flow by various means such as high amplitude forcing [11]. Greenblatt et al [9] compared the active and passive control on an axisymmetric flow. Singh et al [10] compared various active flow techniques on such a flow.

NOMENCLATURE

A	area of the measured region
C_μ	dimensionless momentum coefficient
D	diameter of the circular jet
D_t	turbulent diffusion coefficient
F^+	dimensionless excitation frequency
J	momentum of the jet
M_a	mixing augmentation
Re	Reynolds number
U_0	exit velocity of the jet
ν	viscosity
Γ	circulation
ρ	density of air
u', v', w'	turbulent velocity components
ω_x	dimensionless streamwise vorticity
x, y, z	Cartesian spatial co-ordinates

EXPERIMENTAL SETUP

The wind tunnel used for the experiments is a low speed, circular cross-section, open circuit tunnel with an open-air jet. The exit jet diameter is 90mm and gives a maximum Reynolds number of 90,000 based on jet diameter (Figure 1). The lip of the axisymmetric jet was equipped with a small flap deflected away from the stream at an angle δ . The chord length of the flap was 15mm. The angles used in the investigations were 10°, 20° and 30°. The flap incorporated a flow control slot (15x1.5mm). This slot was connected to a speaker via a flexible tube. A sine-wave was supplied to the speaker to produce the desired frequency and amplitude through which zero mass flux blowing was introduced to the flow.

Different measurement techniques were applied to study the flow field. The control slot was calibrated to get the desired amplitude of the excitations. The velocity measurements were carried out using a Dantec Dynamics 2D Laser Doppler Anemometer (LDA) and stereo PIV.

RESULTS AND DISCUSSION

Investigations were carried out on the jet to quantify the effects of flap deflection angle on the controlled flow. The results were compared based on momentum, streamwise vorticity, circulation and diffusion coefficient. Singh et al [10] provides a theoretical background for the importance of these parameters. Mixing enhancement is related to the circulation and diffusion as follows:

$$\left(\frac{\partial M_a}{\partial(x/\lambda)} \right) \propto \frac{\Gamma^{2/3} D_t^{1/3}}{U_0 \lambda} \quad (1)$$

Here λ represents the “wave-length” between flaps assuming multiple flaps along the perimeter. The diffusion term is separated into two parts in transverse directions:

$$D'_{i,y} \propto \frac{\partial}{\partial y} (\overline{v'q^2}) \quad (2a)$$

$$D'_{i,z} \propto \frac{\partial}{\partial z} (\overline{w'q^2}) \quad (2b)$$

These are then integrated over the area A (Figure 2) to get the two diffusion coefficients:

$$D_{i,y} = \int_A |D'_{i,y}| dydz \quad (3a)$$

$$D_{i,z} = \int_A |D'_{i,z}| dydz \quad (3b)$$

Similarly the circulation is calculated by integrating the streamwise vorticity over the same area:

$$\Gamma = \int_A |\omega_x| dydz \quad (4)$$

As seen from equation 1, in order to have a better mixing behaviour, it is required to have a higher $\Gamma^{2/3} D_t^{1/3}$. The momentum added to the jet using control was quantified by calculating

$$J = \rho \int u^2 dA \quad (5)$$

over the measured area for each case.

Experiments were carried out at a Reynolds number of 25200. The axial position of the measurement plane was $x/D=0.25$ with a reduced frequency $F^+=0.5$. The amplitude of the excitation was quantified by the non dimensional parameter C_μ , the momentum

coefficient. It is defined as the ratio of the momentum added by the control slot to the momentum of the main jet. The amplitude of the excitation was varied from zero (no excitation) to a $C_\mu=0.4\%$.

Figure 3 (a to c) shows the axial velocity contours for the three different flaps at $C_\mu=0.24\%$. The baseline flow is within the diameter of the jet and is not deflected towards the flap. When the control is applied, the flow deflects and attaches to the flap. As the angle is increased from 10° to 30° , this deflection is also increased and a larger area is influenced by the flap. The net increase in momentum for these cases is shown in Figure 4. This is calculated by subtracting the momentum added to the jet by the control slot and taking ratio over the baseline. In all the cases, there is a net increase in jet momentum. As the angle is increased from 10° to 20° , there is a relatively large increase in momentum, especially at the higher amplitudes, where the net increase goes from 1% at 10° to 3.4% at 30° for $C_\mu=0.4\%$. This happens due to the higher entrainment brought about by the increased flap angle. The relatively small difference between the values for 20° and 30° flaps suggests the entrainment saturates and further increase in angle will not be of much use for increase in momentum. Also, going to very high amplitudes might not be desirable. The error bars in the figure represent the maximum relative error in the measurements.

Streamwise vorticity was numerically integrated over the measured area to get the circulation and is shown in Figure 5. As the amplitude increases, the level of circulation also increases. Initially there is a sharp increase but it seems to saturate at amplitude of about 0.3%. It can be seen that as the angle of deflection increases, the overall behaviour remains the same but significantly higher values of circulation are obtained at particular amplitude. It suggests that increase in flap angle helps in generating stronger streamwise vortices.

The turbulent diffusion coefficients were calculated as given by equations 2 and 3. Figure 6 shows the diffusion coefficient along the z-axis. It increase slowly as the amplitude of the excitation increases and saturates at amplitudes about 0.25%. At similar amplitudes, the values for 20° almost double as compared to 10° but this increase is smaller for 30° suggesting that the deflection angle augments the diffusion process but very high angles are not required to achieve the maximum advantage. Diffusion coefficient along the y-axis has similar behaviour (Figure 7), but the diffusion levels are significantly lower than the values along z-axis and very small increase with flap deflection showing that this setup is effective in increasing the radial diffusion.

As given in equation 1, the mixing enhancement varies directly as the product $\Gamma^{2/3} D_t^{1/3}$. These are shown in Figures 8 and 9 for z-axis and y-axis respectively. It also shows a steady increase and then saturation at C_μ of about 0.25% although the values for y-axis are lower owing to lower diffusion coefficient.

CONCLUSIONS

Active flow control of an axisymmetric jet was investigated to have an insight into mechanisms affecting the mixing of the jet flow with the ambient. In the present work, the affect of the flap deflection angle as tested.

- As the control is applied, the jet deflects and attaches to the flap.
- The momentum of the jet increases with increase in angle for the angles tested. This increase strongly depends on the angle of the flap but very high angles will give no further advantage. However, the origin of this increase has to be clarified.

TSFP6 2009

- Strong streamwise vortices and high turbulence intensities were generated. These are highly dependent on the amplitude and the angle of deflection. At higher amplitudes it saturates and further increase in amplitudes does not have any effect.
- The turbulent diffusion is also enhanced by the flap particularly in the radial direction.
- Possibility of an optimal angle of deflection and amplitude is strongly indicated.

FURTHER WORK

The current work is part of an ongoing investigation to look into the various parameters affecting the mixing in jet. Further investigations are being carried out to find out the effects of reduced frequency as well as the effect of having multiple flaps around the perimeter of the nozzle and to test the configuration at compressible speeds.

ACKNOWLEDGEMENT

The authors gratefully acknowledge the financial support for the work provided by the Deutsche Forschungsgemeinschaft (DFG).

REFERENCES

- [1] Greenblatt, D., and Wynanski, I., 2000, "Control of separation by periodic excitation", *Progress in Aerospace Sciences*, 37, pp. 487-545.
- [2] Greenblatt, D., 2005, "Management of vortices trailing flapped wings via separation control," *AIAA Paper* 2005-0061.
- [3] Urzynicok, F., 2003, "Separation control by flow-induced oscillations of a resonator", Ph.D. Dissertation, Technical University of Berlin.
- [4] Gutmark, E., Schadow, K. C., Parr, T. P., Hanson-Parr, D. M., and Wilson, K. J., 1989, "Noncircular jets in combustion systems", *Experiments in Fluids*, 7, pp. 248-258.
- [5] Calkins, F. T., and Butler, G. W., 2004, "Subsonic jet noise reduction variable geometry chevron", *AIAA Paper* 2004-190..
- [6] Pack L. G. and Seifert, A., "Periodic Excitation for Jet Vectoring and Enhanced Spreading," *AIAA Journal of Aircraft*, Vol. 38, No. 3, May-June 2001.
- [7] Waitz, I. A., Elliot, J. K., Fung, A. K. S., Kerwin, J. M., Krasnodebski, J. K., O'Sullivan, M. N., Qiu, Y. J., Tew, D. E., Greitzer, E. M., Marble, F. E., Tan, C. S. and Tillman, T. G., 1997, "Enhanced mixing with streamwise vorticity", *Progress in Aerospace Sciences*, Vol 33, Number 5/6, May/June 1997.
- [8] Greenblatt, D., Singh, Y., Kastantin, Y., Nayeri, C. N., Paschereit, C. O., 2006, "Active management of entrainment and streamwise vortices in an incompressible jet", *Proceedings of the 1st Conference on Active Flow Control*, September 27-29, 2006, Berlin, Germany.
- [9] Mohan, N. K. M., Greenblatt, D., Nayeri, C. N., Paschereit, C. O., Ramamurthi, P. N., "Active and passive flow control of an incompressible axisymmetric jet", *Proceedings of ASME Turbo Expo 2008: Power for Land, Sea and Air*, GT2008, June 9-13, Berlin, Germany, 2008.
- [10] Y. Singh, D. Greenblatt, N. K. Depuru Mohan, C.N. Nayeri and C.O. Paschereit, "Active Control of an Incompressible Axisymmetric Jet", *Proceedings of the 9th Biennial ASME Conference on Engineering Systems Design and Analysis*, ESDA08, July 7-9, 2008, Haifa, Israel.
- [11] Parekh, D. E., Kibens, V., Glezer, A., Wiltse, J. M., and Smith, D. M., 1996, "Innovative jet flow control - mixing enhancement experiments", *AIAA Paper* 96-0308.

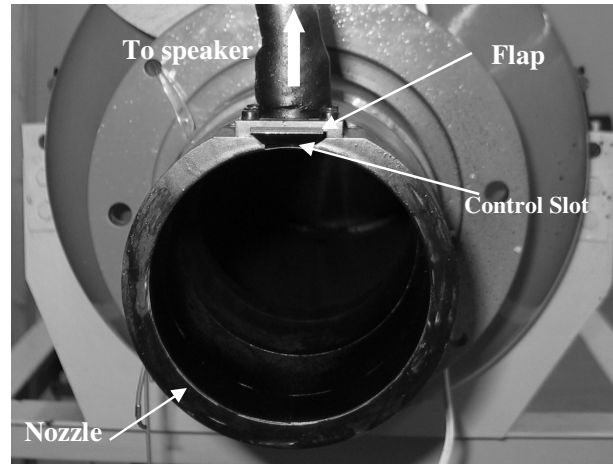


Figure 1: Front view of the nozzle and flap assembly

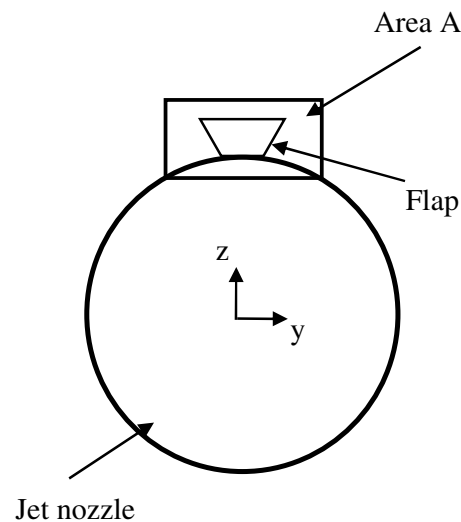


Figure 2: Schematic of the setup showing the axes and the measurement area

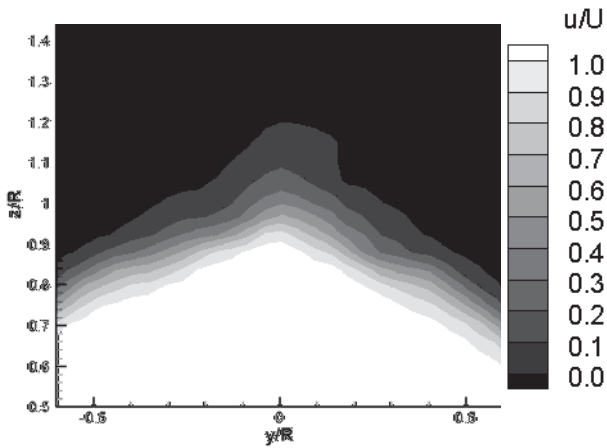


Figure 3a: Axial velocity contour, flap angle 10°

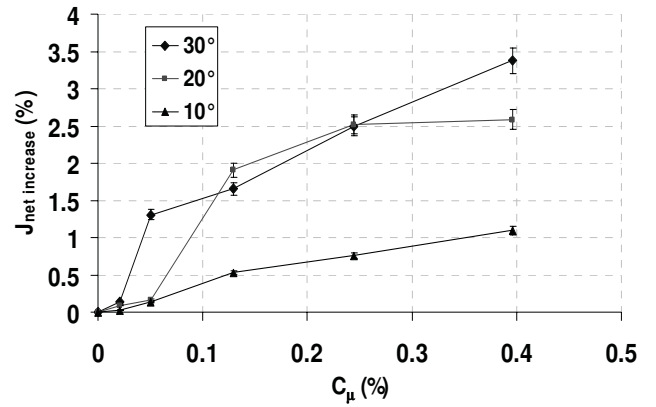


Figure 4: Net momentum increase for the jet

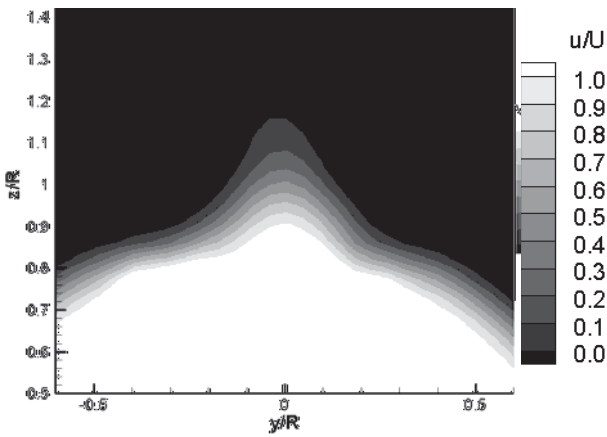


Figure 3b: Axial velocity contour, flap angle 20°

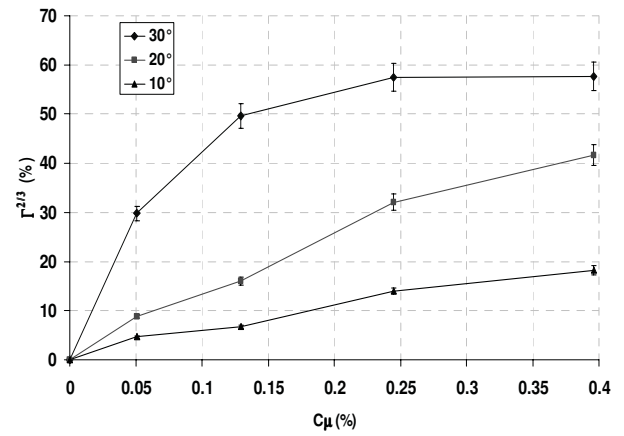


Figure 5: Circulation in the measurement area based on streamwise vorticity

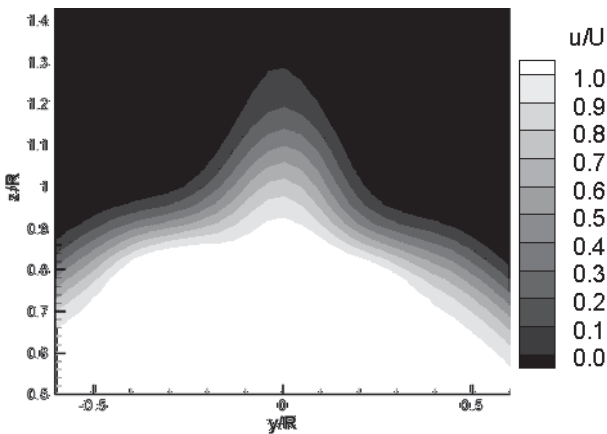


Figure 3c: Axial velocity contour, flap angle 30°

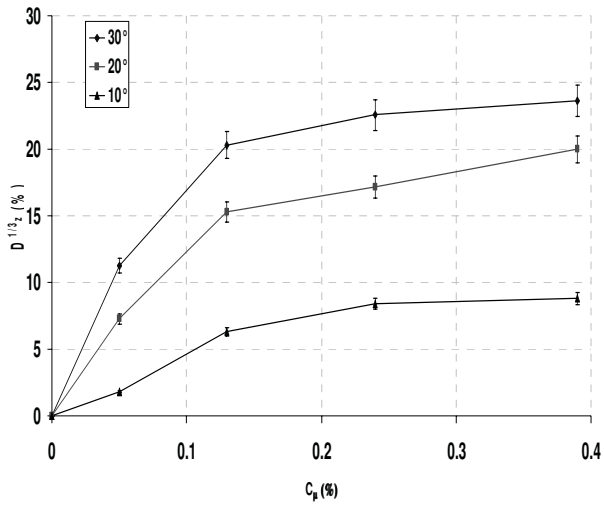


Figure 6: Diffusion coefficient along z-axis

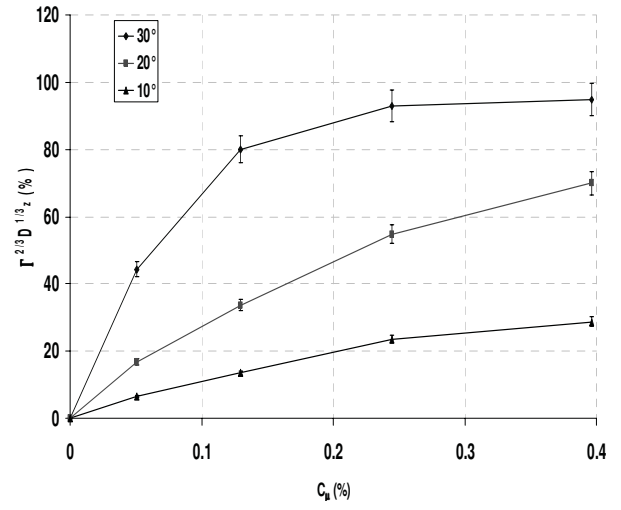


Figure 8: Product of diffusion coefficient and circulation along z-axis

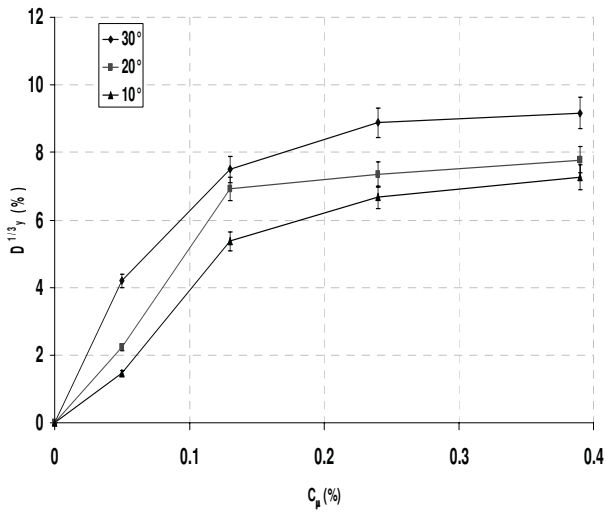


Figure 7: Diffusion coefficient along y-axis

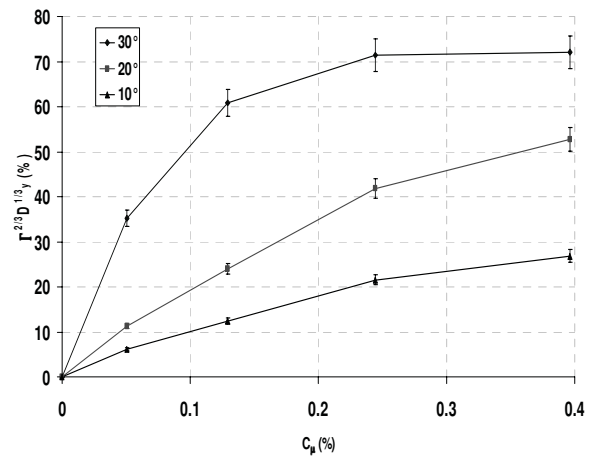


Figure 9: Product of diffusion coefficient and circulation along y-axis